Mon. Not. R. astr. Soc. (1985) **214**, 203–218

Numerical solution of the radiative transfer equation in a magnetized medium

K. N. Nagendra and A. Peraiah *Indian Institute of Astrophysics, Bangalore 560034, India*

Accepted 1984 December 12. Received 1984 December 7; in original form 1984 May 11

Summary. A numerical method of solution based on the discrete space theory of radiative transfer as applied to the transfer problems in an anisotropic medium is discussed. Two simple applications, namely the scattering in the atmosphere of a hot magnetic white dwarf and in a plasma slab immersed in a superstrong magnetic field are discussed. The normal wave transfer equations for the scattering and absorption of radiation are used for this purpose. The solutions are compared with those obtained for the non-magnetic Thomson scattering in the same media. A comparative study is made of the normal wave and Stokes vector equations for a Zeeman active gas.

1 Introduction

The solution of the transfer equation in magneto-active media is of some interest in the computation of the spectrum and polarization of light emitted by many astrophysical sources. There are two approaches to solve this problem. The first consists of solving a system of coupled transfer equations for the Stokes parameters $(IQUV)^{T}$. This method, which is more general, is described in Chandrasekhar (1950) and Unno (1956) for the basic scattering and true absorption problems respectively. For the pure absorption Zeeman lines a number of methods of solution have been proposed (Unno 1956; Stepanov 1958; Beckers 1969; Shipman 1971; Hardorp, Shore & Wittmann 1971; Schmid-Burgk & Wehrse 1976; and Martin & Wickramasinghe 1979, 1981, etc). For a detailed discussion and references on the multiple scattering Stokes vector transfer equations, and various methods of solution, see van de Hulst (1980) and, for applications, Gehrels (1974). The second approach, which is useful for most of the astrophysical plasmas, but less general, is the 'polarization normal wave representation' which is a special case of the general density matrix formulation of the transfer equation (Ginzburg 1964; Dolginov, Gnedin & Silant'ev 1970; Zheleznyakov 1970; Lamb & ter Haar 1971, etc.). A slightly different approach is taken in Pacholczyk (1977) and Melrose (1980). For recent references on the applications of this method see Meszaros (1984).

2 Polarization normal wave transfer equations

The radiation polarization density matrix (transfer) equations have been discussed in detail in Dolginov *et al.* (1970) for arbitrary anisotropic media. For the general arguments leading from these equations to the normal wave equations see Gnedin & Pavlov (1974). The transfer equation for the intensities of elliptically polarized normal waves ($j = 1$, extraordinary wave and $j = 2$, ordinary wave) is given by

$$\mu \frac{dI_j}{\rho dZ} = -\alpha_j I_j + \sum_k \int_{-1}^{+1} \frac{d\sigma_{jk}(\xi, \xi')}{d\xi} I_k(\xi')\, d\xi' + k_j \frac{B}{2}. \tag{1}$$

Azimuthal symmetry and coherent scattering are implied. $\mu = \cos\theta \in (-1, +1)$, θ is the angle between the ray and the Z-axis, the symmetry axis of the medium. $\xi = \cos\psi$ where ψ = angle between the ray and the magnetic field, and χ is the field azimuth in an orthogonal system with the ray going along the z-axis. ρ is the mass density and $\alpha_j = (\sigma_j + k_j)$ is the mass extinction coefficient. $d\sigma_{jk}(\xi, \xi')/d\xi$ is the azimuthally symmetric differential 'mode conversion scattering' coefficient ($j \leftarrow k$) and $k_j B/2$ is the thermal emission coefficient with B the Planck function.

The cold plasma scattering cross-sections have been calculated by a number of authors (see e.g. Canuto, Lodenquai & Ruderman 1971; Gnedin & Sunyaev 1974a; Ventura 1979, etc.). We employ the expressions in the form given by Kaminker, Pavlov & Shibanov (1982)

$$\frac{d\sigma_{jk}(\xi, \xi')}{d\xi} = \frac{3}{4}\left(\frac{N_e \sigma_T}{\rho}\right) \sum_{\alpha=-1}^{+1} t_\alpha^2 a_\alpha^j(\xi) a_\alpha^k(\xi'), \tag{2}$$

where $t_\alpha = (1 + \alpha\sqrt{u})$; $\sqrt{u} = \omega_c/\omega = eB/mc\omega$ and the scattering amplitudes are

$$a_0^j(\xi) = \frac{1-\xi^2}{2}(1 + P_Q^j); \quad a_{\pm 1}^j(\xi) = \tfrac{1}{4}\left[1 + \xi^2 \pm 2P_V^j \xi - P_Q^j(1-\xi^2)\right], \tag{3}$$

satisfying the completeness and transversality conditions (Ventura 1979)

$$\sum_{j=1,2} a_\pm^j(\xi) = \frac{1+\xi^2}{2}; \quad \sum_{j=1,2} a_0^j(\xi) = 1-\xi^2; \quad \sum_{\alpha=-1}^{+1} a_\alpha^j(\xi) = 1, \tag{4}$$

$$P_Q^j = (-1)^j \frac{|q|}{\sqrt{1+q^2}}; \quad P_V^j = (-1)^j \frac{\mathrm{sgn}\,(q)}{\sqrt{1+q^2}}; \quad q = \frac{1-\xi^2}{2\xi} \cdot \frac{\omega_c}{\omega}. \tag{5}$$

The 'integrated' scattering coefficients are given by

$$\sigma_j(\xi) = \sum_{k=1,2} \sigma_{jk}(\xi) = \sigma_{j1}(\xi) + \sigma_{j2}(\xi) = \left(\frac{N_e \sigma_T}{\rho}\right) \sum_{\alpha=-1}^{+1} t_\alpha^2 a_\alpha^j(\xi), \tag{6}$$

The absorption coefficients for the normal waves are $k_j = k_j^{bf} + k_j^{ff} + \ldots$. We give below only those which are important for our purposes.

2.1 FREE–FREE ABSORPTION COEFFICIENTS

The mass absorption coefficient for an ion of charge (Ze) is given by

$$k_j^{ff}(\xi) = \frac{1}{\rho} \sum_{\alpha=-1}^{+1} t_\alpha^2 \zeta^{(\alpha)} a_\alpha^j(\xi), \tag{7}$$

where $\zeta^{(\alpha)}$ is the true linear absorption coefficient for the αth component, of the cyclic projection (of the medium polarizability tensor) $e^j_\alpha(\xi)$ (Kaminker *et al.* 1982).

$$\left.\begin{aligned}\zeta^{(+1)} = \zeta^{(-1)} \equiv \zeta_\perp = \nu_\perp/\nu \\ \zeta^{(0)} = \zeta_\parallel \equiv \nu_\parallel/\nu\end{aligned}\right\}, \tag{8}$$

where the longitudinal (wrt$B$) and transverse effective collision frequencies are given by (see Pavlov & Panov 1976; Ventura 1973; Nagel & Ventura 1983)

$$\nu_{\parallel,\perp} = \left(\frac{2\pi}{m}\right)^{1/2} \frac{N_i Z^2 e^4}{(kT)^{3/2}} \frac{kT}{\hbar\omega} \left(1 - \exp\left[-(\hbar\omega/kT)\right]\right) g_{\parallel,\perp}. \tag{9}$$

The radiative width

$$\nu_\gamma = 2e^2\omega^2/3mc^3. \tag{10}$$

The magnetic Gaunt factors $g_{\parallel,\perp}$ exhibit resonances at $s\omega_c$ ($s = 1, 2, 3, \ldots$). In the present computations we have employed $g_{\parallel,\perp} \equiv g$, the non-magnetic Gaunt factor, which is a good approximation for $\omega_c \ll \omega$.

2.2 BOUND–FREE ABSORPTION COEFFICIENTS

They also undergo resonances at $s\omega_c$ ($s = 1, 2, 3, \ldots$). For weaker fields ($\omega_c \ll \omega$), an expression given by Pavlov (1973) in the hydrogenic approximation can be used

$$k^{bf}_j(\xi) = \left(\frac{k^{\mathrm{obf}}}{\rho}\right)\left[1 + \frac{3}{4}\left(\frac{\omega_c}{\Delta\omega}\right)^{3/2} f(x,a)\, A_j(\xi)\right], \tag{11}$$

where k^{obf} is the zero field linear absorption coefficient.

$$x = \frac{\delta\omega}{\omega_c} = \frac{\Delta\omega - N\omega_c}{\omega_c} = \left[\frac{\hbar\omega - E_n}{\hbar\omega_c} - \frac{1}{2}\right] - N = D - N, \tag{12}$$

where N = Integral (D). Therefore $0 \leqslant x \leqslant 1$.

$$a = \Gamma_D/\omega_c = \frac{\omega}{\omega_c}\sqrt{\frac{kT}{Mc^2}}, \tag{13}$$

M = mass of the emitting atom. The profile function $f(x, a)$ which is a periodic function with period unity is given by

$$f(x, a) = \frac{1}{a\sqrt{\pi}} \sum_{k=-\infty}^{+\infty} \int_0^{+1} y^{-1/2} \exp\left[-(x - y - k)^2/a^2\right] dy. \tag{14}$$

In the dipole approximation the absorption amplitudes $A_i(\xi)$ are given by

$$A_1(\xi) = \xi^2; \qquad A_2(\xi) = 1. \tag{15}$$

$$E_n = I_{\mathrm{H}}(1 - 1/n^2), \qquad I_{\mathrm{H}} \simeq 21.36 \times 10^{-12}\,\mathrm{ergs}, \tag{16}$$

where n is the principal quantum number. In our case (the Paschen continuum), $n = 3$. In hot white dwarf atmospheres, this source of opacity does not contribute significantly to the continuum polarization. The H^- ion opacities for normal waves have been calculated in the same level of approximation by Pavlov (1973); these are useful for cool white dwarfs.

The Stokes parameters can be computed from the normal wave intensities by using ($j = 1, 2$)

$$I = \sum_j I_j; \qquad Q = \sum_j P^j_Q I_j; \qquad U = \sum_j P^j_U I_j = 0; \qquad V = \sum_j P^j_V I_j; \tag{17}$$

for azimuthally symmetric problems, $P^j_U \equiv 0$, $U \equiv 0$.

3 A brief description of the method of solution

We indicate below how a simple computing algorithm can be derived for solving the normal wave or Stokes vector transfer equations in a magnetized plasma. In this treatment, which is an extension of the discrete space theory of radiative transfer (Grant & Hunt 1968a, 1969a, b; Peraiah 1984), the difference equations are derived by a discrete ordinate method and solved. First we write the transfer equation (1) in matrix form, as

$$\mu \frac{d\mathbf{I}(-\mu)}{d\tau} = \mathbf{A}(\mu)\mathbf{I}(\mu) - \left\{ \bar{\omega} \int_{-1}^{+1} \mathbf{P}(\mu, \mu')\mathbf{I}(\mu')\, d\mu' + (1 - \bar{\omega})\, \mathbf{A}_a(\mu)\mathbf{B}(\mu) \right\}$$
$$- \bar{\omega}\, \mathbf{P}_*(\mu, \mu_0)\mathbf{I}_*(\mu_0) \exp(-\tau/\mu_0), \tag{18}$$

$$-\mu \frac{d\mathbf{I}(-\mu)}{d\tau} = \mathbf{A}(-\mu)\mathbf{I}(-\mu) - \left\{ \bar{\omega} \int_{-1}^{+1} \mathbf{P}(-\mu, \mu')\mathbf{I}(\mu')\, d\mu' + (1 - \bar{\omega})\, \mathbf{A}_a(-\mu)\mathbf{B}(-\mu) \right\}$$
$$- \bar{\omega}\, \mathbf{P}_*(-\mu, \mu_0)\mathbf{I}_*(\mu_0) \exp(-\tau/\mu_0), \tag{19}$$

where $\mu \in (0, 1)$, and $\mathbf{B}(\mu)$ is taken as generally anisotropic.

The last terms on the rhs in equations (18) and (19) represent the contribution to the source function due to the directly transmitted beam $\mathbf{I}_*(\mu_0)$ in the direction μ_0 incident on the free surface ($\tau = 0$) of the medium. Equations (18) and (19) represent the rays in the upper and lower half space of angles respectively, wrt the optical depth scale, increasing into the atmosphere. In the continuous case, each one of the equations above is a matrix equation with $\mathbf{A}$ and $\mathbf{P}$ being (2×2) matrices and $\mathbf{I}$ and $\mathbf{B}$ (2×1) vectors. The optical depth scale $d\tau = -(k^C + \sigma_T)\rho\, dZ$ is defined wrt the zero field extinction coefficient. The $\mathbf{A}$ matrices are defined as

$$\mathbf{A}^{\pm} = \bar{\omega}\mathbf{A}^{\pm}_s + (1 - \bar{\omega})\mathbf{A}^{\pm}_a; \qquad \bar{\omega} = \frac{\sigma_T}{\sigma_T + k^C}, \qquad \mathbf{A}^{\pm} = \mathbf{A}(\pm\mu), \tag{20}$$

$$\mathbf{A}^{\pm}_s = \frac{1}{\sigma_T}\begin{bmatrix} \sigma^{\pm}_1 & 0 \\ 0 & \sigma^{\pm}_2 \end{bmatrix}; \qquad \mathbf{A}^{\pm}_a = \begin{bmatrix} k^{\pm}_1 & 0 \\ 0 & k^{\pm}_2 \end{bmatrix}, \qquad \left.\begin{array}{l} \mathbf{A}^{\pm} = \mathbf{A}_a(\pm\mu) \\ \mathbf{A}^{\pm}_s = \mathbf{A}_s(\pm\mu) \end{array}\right\} \tag{21}$$

's' and 'a' denote the scattering and true absorptions $\bar{\omega}$ is the albedo for single scattering ($0 \leqslant \bar{\omega} \leqslant 1$). The scattering phase matrix defined as

$$\mathbf{P}(\mu, \mu') = \frac{1}{\sigma_T}\frac{d\sigma_{jk}(\xi, \xi')}{d\xi} = \frac{1}{\sigma_T}\frac{d}{d\xi}\begin{bmatrix} \sigma_{11}(\xi, \xi') & \sigma_{12}(\xi, \xi') \\ \sigma_{21}(\xi, \xi') & \sigma_{22}(\xi, \xi') \end{bmatrix}, \tag{22}$$

satisfies the normalization

$$\frac{1}{2}\int_{-1}^{+1} \mathbf{P}(\mu, \mu')\, d\mu' = 1; \qquad -1 \leqslant \mu, \mu' \leqslant +1. \tag{23}$$

This scattering integral source term gives rise to a diffuse radiation field. The second term in the flower brackets is the 'internal thermal emission' source term. The intensity and the anisotropic thermal source vector are written as

$$\mathbf{I}(\pm\mu) = \begin{bmatrix} I_1(\pm\mu) \\ I_2(\pm\mu) \end{bmatrix}; \qquad \mathbf{B}(\pm\mu) = \begin{bmatrix} B(\pm\mu)/2 \\ B(\pm\mu)/2 \end{bmatrix}; \qquad \left.\begin{matrix} \mathbf{I}^{\pm} = \mathbf{I}(\pm\mu) \\ \mathbf{B}^{\pm} = \mathbf{B}(\pm\mu) \end{matrix}\right\} \tag{24}$$

Now, the 'discrete ordinate' forms of equations (18) and (19) are written, in matrix form, as

$$\mathbf{M}\frac{d\mathbf{I}^{+}}{d\tau} = \mathbf{A}^{+}\mathbf{I}^{+} - \{\bar{\omega}[\mathbf{P}^{++}\mathbf{G}\mathbf{I}^{+} + \mathbf{P}^{+-}\mathbf{G}\mathbf{I}^{-}] + (1-\bar{\omega})\mathbf{A}_a^{+}\mathbf{B}^{+}\}$$
$$- \bar{\omega}\mathbf{P}_{*}^{++}\mathbf{I}_{*}^{+}\exp(-\tau/\mu_0) \tag{25}$$

$$-\mathbf{M}\frac{d\mathbf{I}^{-}}{d\tau} = \mathbf{A}^{-}\mathbf{I}^{-} - \{\bar{\omega}[\mathbf{P}^{-+}\mathbf{G}\mathbf{I}^{+} + \mathbf{P}^{--}\mathbf{G}\mathbf{I}^{-}] + (1-\bar{\omega})\mathbf{A}_a^{-}\mathbf{B}^{-}\}$$
$$- \bar{\omega}\mathbf{P}_{*}^{-+}\mathbf{I}_{*}^{+}\exp(-\tau/\mu_0), \tag{26}$$

where the signs in the superscript indicate the signs attached to $|\mu|$ in the respective physical quantities.

$$\mathbf{M} = \begin{bmatrix} M' & 0 \\ 0 & M' \end{bmatrix}; \qquad \mathbf{G} = \begin{bmatrix} G' & 0 \\ 0 & G' \end{bmatrix}; \qquad \left.\begin{matrix} M' = (M_{jk}) = \mu_j\delta_{jk} \\ G' = (G_{jk}) = c_j\delta_{jk} \end{matrix}\right\} j,\ k = 1, 2 \ldots J, \tag{27}$$

$$\mathbf{P}^{++} = \begin{bmatrix} P_{11}^{++} & P_{12}^{++} \\ P_{21}^{++} & P_{22}^{++} \end{bmatrix}; \qquad \left.\begin{matrix} P_{\alpha\beta}^{++} = P_{\alpha\beta}(\mu_j, \mu_k) = P_{\alpha\beta}^{--} \\ P_{\alpha\beta}^{+-} = P_{\alpha\beta}(\mu_j, -\mu_k) = P_{\alpha\beta}^{-+} \end{matrix}\right\} \begin{matrix} \alpha, \beta = 1, 2 \\ \mu_j, \mu_k > 0 \end{matrix}, \tag{28}$$

with similar expressions for $\mathbf{P}^{--}$, $\mathbf{P}^{+-}$ and $\mathbf{P}^{-+}$. J is the order of the quadrature formula which is used for angular discretization. Hence all the matrices are now of dimension $(2J \times 2J)$ and the vectors are of dimension $(2J \times 1)$. The matrices $\mathbf{P}_{*}^{+-}$ and $\mathbf{P}_{*}^{--}$ and $\mathbf{I}_{*}^{+}$ are given by

$$\mathbf{P}_{*}^{++} = \begin{bmatrix} P_{11*}^{++} & P_{12*}^{++} \\ P_{21*}^{++} & P_{22*}^{++} \end{bmatrix}; \qquad \left.\begin{matrix} P_{\alpha\beta*}^{++} = P_{\alpha\beta*}(\mu_j, \mu_0\delta_{k1}) = P_{\alpha\beta*}^{--} \\ P_{\alpha\beta*}^{-+} = P_{\alpha\beta*}(-\mu_j, \mu_0\delta_{k1}) = P_{\alpha\beta*}^{+-} \end{matrix}\right\} \begin{matrix} \alpha, \beta = 1, 2 \\ \mu_j > 0 \end{matrix}, \tag{29}$$

$$\mathbf{I}_{*}^{+} = [I_*(\mu_0)\delta_{k1}, \quad I_*(\mu_0)\delta_{k1}]^{\mathrm{T}}, \quad k = 1, 2, \ldots J.$$

Integrating the matrix equations (29) and (30) over a 'cell' bounded by the planes τ_n and τ_{n+1}, we get

$$\mathbf{M}[\mathbf{I}_{n+1}^{+} - \mathbf{I}_{n}^{+}] = \Delta\tau\mathbf{A}_{n+1/2}^{+}\mathbf{I}_{n+1/2}^{+} - \Delta\tau$$
$$\times \{\bar{\omega}_{n+1/2}[\mathbf{P}_{n+1/2}^{++}\mathbf{G}\mathbf{I}_{n+1/2}^{+} + \mathbf{P}_{n+1/2}^{+-}\mathbf{G}\mathbf{I}_{n+1/2}^{-}] + \bar{\omega}_{n+1/2}\mathbf{P}_{*n+1/2}^{++}\mathbf{I}_{*}^{+}$$
$$\times \frac{\exp(-\tau_n/\mu_0)}{2}[\exp(-\Delta\tau/\mu_0) + 1] + (1-\bar{\omega}_{n+1/2})\mathbf{A}_{a,\,n+1/2}^{+}\mathbf{B}_{n+1/2}^{+}\}, \tag{31}$$

$$-\mathbf{M}[\mathbf{I}_{n+1}^{-} - \mathbf{I}_{n}^{-}] = \Delta\tau\mathbf{A}_{n+1/2}^{-}\mathbf{I}_{n+1/2}^{-} - \Delta\tau$$
$$\times \{\bar{\omega}_{n+1/2}[\mathbf{P}_{n+1/2}^{-+}\mathbf{G}\mathbf{I}_{n+1/2}^{+} + \mathbf{P}_{n+1/2}^{--}\mathbf{G}\mathbf{I}_{n+1/2}^{-}] + \bar{\omega}_{n+1/2}\mathbf{P}_{*n+1/2}^{-+}\mathbf{I}_{*}^{+}$$
$$\times \frac{\exp(-\tau_n/\mu_0)}{2}[\exp(-\Delta\tau/\mu_0) + 1] + (1-\bar{\omega}_{n+1/2})\mathbf{A}_{a,\,n+1/2}^{-}\mathbf{B}_{n+1/2}^{-}\}, \tag{32}$$

with $\mathbf{I}_n^{\pm} \equiv \mathbf{I}^{\pm}(\tau_n)$; $\mathbf{I}_{n+1}^{\pm} \equiv \mathbf{I}^{\pm}(\tau_{n+1})$, $n = 1, 2, \ldots N$, where N = number of shells into which the atmosphere is divided. The suitable cell averages based on the diamond scheme (see Grant & Hunt 1968a) are explicitely used in writing equations (31) and (32). The subscript $n + \frac{1}{2}$ denotes such averages, for example $\bar{\omega}_{n+\frac{1}{2}} = (\bar{\omega}_{n+1} + \bar{\omega}_n)/2$ and so on. The last term is written by cell averaging the dilution coefficient $\exp(-\tau/\mu_0)$ of the direct beam $\mathbf{I}_*^+$ over the given cell. We take $\Delta\tau = (k^C + \sigma_T)_{n+\frac{1}{2}} \cdot \rho_{n+\frac{1}{2}}(Z_n - Z_{n+1}) = \tau_{n+1} - \tau_n$. Making use of the expressions

$$\mathbf{I}_{n+1/2}^{\pm} = {}^1/_2(\mathbf{I}_{n+1}^{\pm} + \mathbf{I}_n^{\pm}), \tag{33}$$

we can re-arrange equations (31) and (32) in a canonical form as

$$\begin{bmatrix} \mathbf{I}_{n+1}^{+} \\ \mathbf{I}_n^{-} \end{bmatrix} = \begin{bmatrix} \mathbf{t}(n+1, n) & \mathbf{r}(n, n+1) \\ \mathbf{r}(n+1, n) & \mathbf{t}(n, n+1) \end{bmatrix} \begin{bmatrix} \mathbf{I}_n^{+} \\ \mathbf{I}_{n+1}^{-} \end{bmatrix} + \begin{bmatrix} \boldsymbol{\Sigma}_{n+1/2}^{+} \\ \boldsymbol{\Sigma}_{n+1/2}^{-} \end{bmatrix}. \tag{34}$$

This straightforward, but tedious elimination can be cast in the form of a computing algorithm which we have given in the Appendix. The operators $\mathbf{r}$ and $\mathbf{t}$ appearing in the canonical form (34) have a physical interpretation as matrix operators for diffuse reflection and transmission respectively, of the radiation incident on the shell between the planes τ_n and τ_{n+1}. Similarly the vector operators $\boldsymbol{\Sigma}_{n+\frac{1}{2}}$ represent the radiation which emerges from the surfaces of the shell due to internal emission sources plus the diluted directly transmitted beam.

A computational note: The procedure is based on the computation of $\mathbf{r}$, $\mathbf{t}$ and $\boldsymbol{\Sigma}$ operators of all the N shells, into which we have divided the medium. We have explicitly assumed in deriving equations (31) and (32) that the stability and non-negativity of the cell operators, and hence of the specific intensity vectors, is assured, for a value of the shell thickness $\Delta\tau \leqslant \tau_{\text{crit}}$. τ_{crit} is the 'local critical optical depth' which is actually calculated by requiring that $\mathbf{S}^{+-} \geqslant 0$, $\mathbf{s}^{-+} \geqslant 0$ and $\boldsymbol{\Delta}^{\pm} \geqslant 0$. For a large class of scattering problems one can use the expression

$$(\tau_{\text{crit}})_n = \operatorname{Min}_j \left[\frac{2\mu_j}{[1 - \bar{\omega}_{n+1/2} \mathbf{P}_{n+1/2}^{++}(\mu_j, \mu_j')\, c_j]} \right], \tag{35}$$

to compute this value. If $\Delta\tau > \tau_{\text{crit}}$, the shell is further sub-divided, and the $\mathbf{r}$, $\mathbf{t}$ and $\boldsymbol{\Sigma}$ operators of the composite thick shell can be generated by a fast doubling algorithm (Grant & Hunt 1969b). A convenient test of the accuracy of the solution is offered by the requirement of 'global flux conservation' – the outgoing flux should equal the incident flux for a 'conservative' scattering atmosphere ($\bar{\omega} \equiv 1$). It is shown in Grant & Hunt (1969b) and Peraiah & Grant (1973) that this criterion is always satisfied provided care is taken to ensure that the scattering phase matrix is normalized to a high degree of accuracy. Consequently, it is preferable that a finer angular discretization is employed, particularly for the strong field scattering phase matrices which are highly anisotropic. A complete discussion of these aspects, namely the spatial and angular discretization and flux conservation in the finite difference schemes, can be found in Wiscombe (1976a, b). Since the recursive algorithm used for computing the internal and emergent radiation fields is the same as that given in Grant & Hunt (1968b) and Peraiah (1984); we do not repeat them here. However, the $\mathbf{r}$, $\mathbf{t}$ and $\boldsymbol{\Sigma}$ operators should now be computed from the algorithm given in the Appendix, along with the relevant boundary conditions which are specified based on the problem.

4 Useful limiting cases and applications

4.1 ZERO FIELD LIMIT OF THE COLD PLASMA NORMAL WAVE TRANSFER EQUATIONS

This can be obtained by substituting the magnetic field strength $B = 0$ ($u \doteq 0$: $q = 0$: $P_Q^j = 0$; $P_V^j = \mp 1$; $t_\alpha = 1$; $\alpha = 0, \pm 1$, $j = 1, 2$). Since there is no preferred direction in the medium which is isotropic, we can take $\xi \equiv \mu$. The normal waves $I_{1,2} = (I \mp V)/2$ are now circularly polarized, with the Z-axis, normal to the atmosphere, being the physically distinguished direction. From the normal wave equation (1) we finally get

$$\mu \frac{d}{d\tau}\begin{bmatrix} I(\mu) \\ V(\mu) \end{bmatrix} = \begin{bmatrix} I(\mu) \\ V(\mu) \end{bmatrix} - \frac{3}{16}\bar{\omega}\int_{-1}^{+1}\begin{bmatrix} 3-\mu^2+(3\mu^2-1)\mu'^2 & 0 \\ 0 & 4\mu\mu' \end{bmatrix}\begin{bmatrix} I(\mu') \\ V(\mu') \end{bmatrix} \times d\mu' - (1-\bar{\omega})\begin{bmatrix} B \\ 0 \end{bmatrix}. \tag{36}$$

Notice that these equations can also be obtained from the Stokes vector equations of Chandrasekhar by taking $I_{l,r} = I/2$ in the azimuth-independent part of the phase matrix. The first equation is simply the transfer equation for Rayleigh phase function (see Chandrasekhar 1950, p. 17). So this case can be used as a check on the correct programming of the algorithm, since the tabulated solutions for this standard problem are available, e.g. van de Hulst (1980).

4.2 LIMITING CASE OF SUPERSTRONG MAGNETIC FIELDS

If we have a situation where $\omega \ll \omega_c$, for example the optical range and the magnetic field $B \gg 10^8$ G, the normal waves are characterized by a large linear polarization over a wide range of angles ξ. For this case ($u \gg 1$; $q \gg 1$; $P_Q^j \cong \mp 1$; $P_V^j \cong 0$; $t_{\pm 1} = 0$, $t_0 = 1$; $j = 1, 2$), we get the following transfer equations

$$\mu \frac{dI_1(\mu)}{d\tau} \simeq 0, \qquad \text{or} \qquad I_1 = \text{constant}, \tag{37}$$

$$\mu \frac{dI_2(\mu)}{d\tau} \simeq 2(1-\xi^2)I_2(\mu) - \bar{\omega}\frac{3}{4}\int_{-1}^{+1}(1-\xi^2)(1-\xi'^2)I_2(\xi')\,d\mu' - (1-\bar{\omega})(1-\xi^2)\frac{B}{2}, \tag{38}$$

$\xi = \xi(\mu)$, $\xi' = \xi'(\mu')$. It is interesting to note that the ordinary wave equation (38) is independent of the field strength. In particular, for quasi-transverse propagation, the electric vector vibrates in directions almost parallel to the field lines, which is responsible for the little influence of the field on the electron oscillations. The absorption and scattering coefficients are nearly equal to their field-free values. As far as the extraordinary wave is concerned, these coefficients become extremely small compared to the ordinary wave. Therefore the radiative transfer hardly changes the value of I_1, which remains constant according to equation (37).

4.3 POLARIZATION OF RADIATION IN THE ATMOSPHERES OF HOT MAGNETIC WHITE DWARFS AND MAGNETIZED NEUTRON STARS

Recently two hot magnetic white dwarfs have been discovered by Liebert *et al.* (1983). In the atmospheres of such stars, scattering plays a significant role at lower optical depths. In

weaker magnetic fields ($\omega_c \ll \omega$; $B \sim 10^7$ G and optical wavelengths), the transfer coefficients do not differ much from the non-magnetic values. So the polarization is in general very small, and $p \sim q^2$.

In Fig. 1 the angular distribution of the emergent I, p and q are shown when isotropic radiation is incident at τ_{max} given by $I_j^-(\tau_{max}) = B(\tau_{max})/2$ and no radiation is incident on the top of the atmosphere; these are the boundary conditions. The angular distributions of I are almost similar for all the cases, namely $\Theta_B = 0$, $\pi/4$, $\pi/2$, with the emergent intensity in general increasing by a very small amount (~ 1 per cent). But p and q are more sensitive wrt the angle Θ_B. The angular distributions for $\bar{\omega} = 0$ and $\bar{\omega} = \bar{\omega}(\tau)$ do not differ very much because the 'partial' angular dependence has already entered through k_j in the former case also. The effect of external illumination $[I_j^+(\tau = 0) \neq 0]$ on the free surface along with the

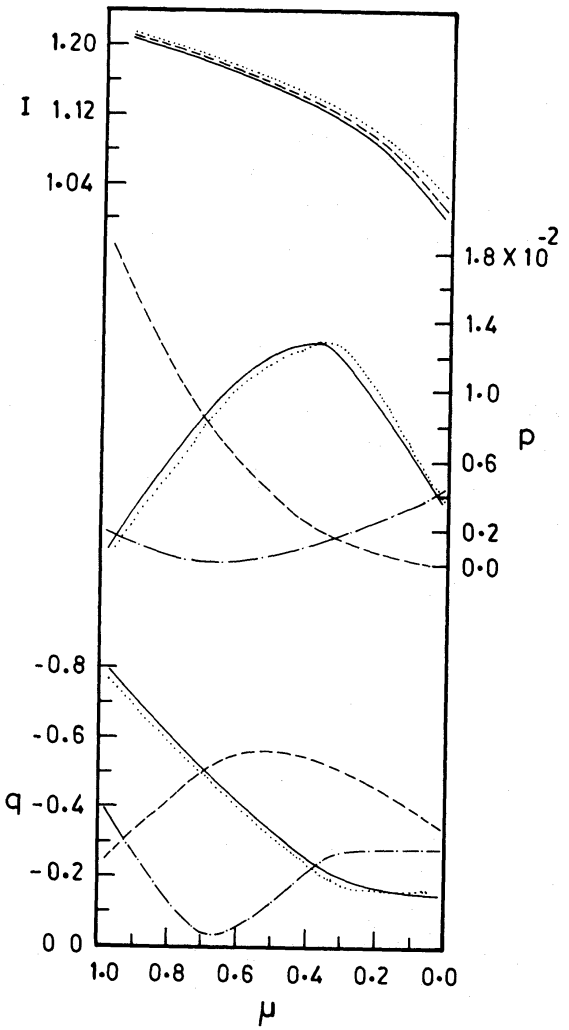

Figure 1. Angular distribution of the emergent intensity I (in the units of $B(T_0)$, T_0 = surface temperature), percentage linear polarization $p(=Q/I)$ and circular $q(=V/I)$ polarizations computed using a realistic model atmosphere of a hot pure hydrogen white dwarf (T_{eff} = 50 000 K, log g = 8) taken from Wesemael *et al.* (1980). The field strength is set at $B = 5 \times 10^6$ G. An eight-point Gauss quadrature is used in the angular discretization. The transfer equations are integrated up to $\tau \simeq 22$. Full lines: ($\Theta_B = 0$), where Θ_B is the angle between the field B and the normal Z to the plane parallel atmospheric layers. Dot-dash lines: ($\Theta_B = \pi/4$), dash lines: ($\Theta_B = \pi/2$). The dotted lines represent the special case of the magneto-absorption ($\bar{\omega} \equiv 0$). The intensity distributions for $\Theta_B = 0$ and $\Theta_B = \pi/4$ are not resolved in the adopted scale.

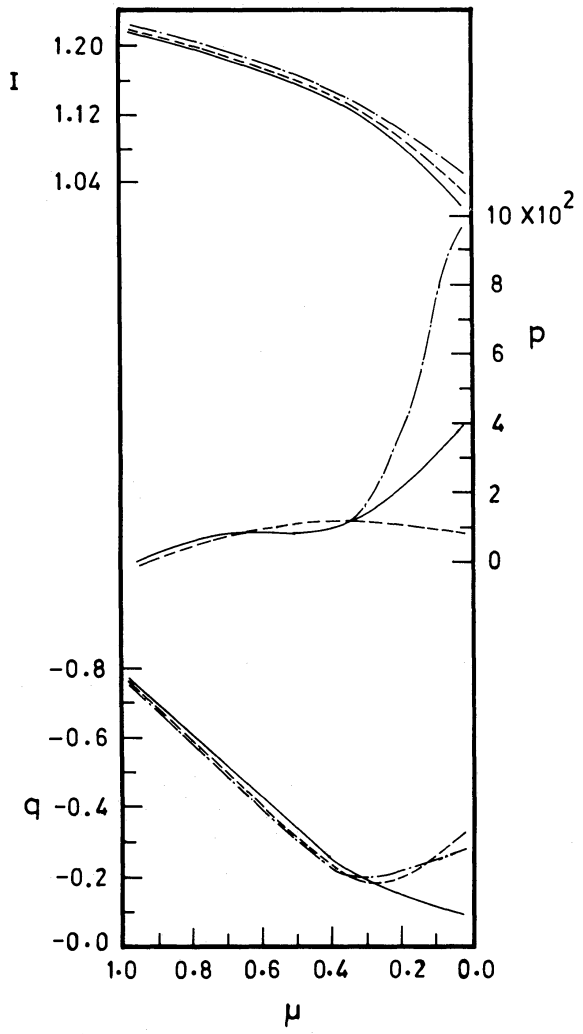

Figure 2. As Fig. 1, but showing the effect on I, p and q, of an external illumination on the top surface $\tau = 0$, along with an input at $\tau = \tau_{max}$. For all cases, $\Theta_B = 0$. Full lines: an isotropic low-temperature irradiance given by $I_j(\mu) = B(T_0)/2$, $j = 1, 2$. Dashed lines: an external illumination distributed as $\cos\theta$, i.e. $I_j(\mu) = [B(T_0)/2]\mu$, $\mu = \cos\theta$. Dot-dash lines: a high-temperature external irradiance $I_j(\mu) = [B(T = 75\,000\,\mathrm{K})/2]\mu$, an arbitrary change in the temperature gradient obtained by enhancing the local temperature continuously, from 1 per cent at $\tau = 10^{-4}$ to 11 per cent at $\tau = 0$, thus changing the source function gradient.

inner boundary condition is shown in the Fig. 2. For isotropic illumination, p is enhanced by a large amount, particularly for transverse directions ($\Theta_B = 0$; $\theta = \pi/2$), while q is only slightly reduced. For an anisotropic unpolarized diffuse external irradiance (not the direct beam), the value of p increases, but its relative importance near the limb is suppressed because of the angular dependence of the incident radiation, which dominates that of the emergent radiation field. q increases near the limb for the same reason. The effect of altering the normal 'source function gradient', by irradiating a high-temperature ambient radiation at $\tau = 0$, is again larger on the p values in the transverse directions than on q. In general, the circular polarization q is proportional to the 'temperature gradient' in a high-temperature atmosphere, unlike the case of a cooler medium where it is proportional to the radiative flux gradient (see Gnedin & Sunyaev 1974b; Kaminker *et al.* 1982).

In Fig. 3(a) we have shown the relative intensities of the extraordinary (ext) and ordinary (ord) modes, for a 'self emitting' plasma slab whose parameters are representative of a polar

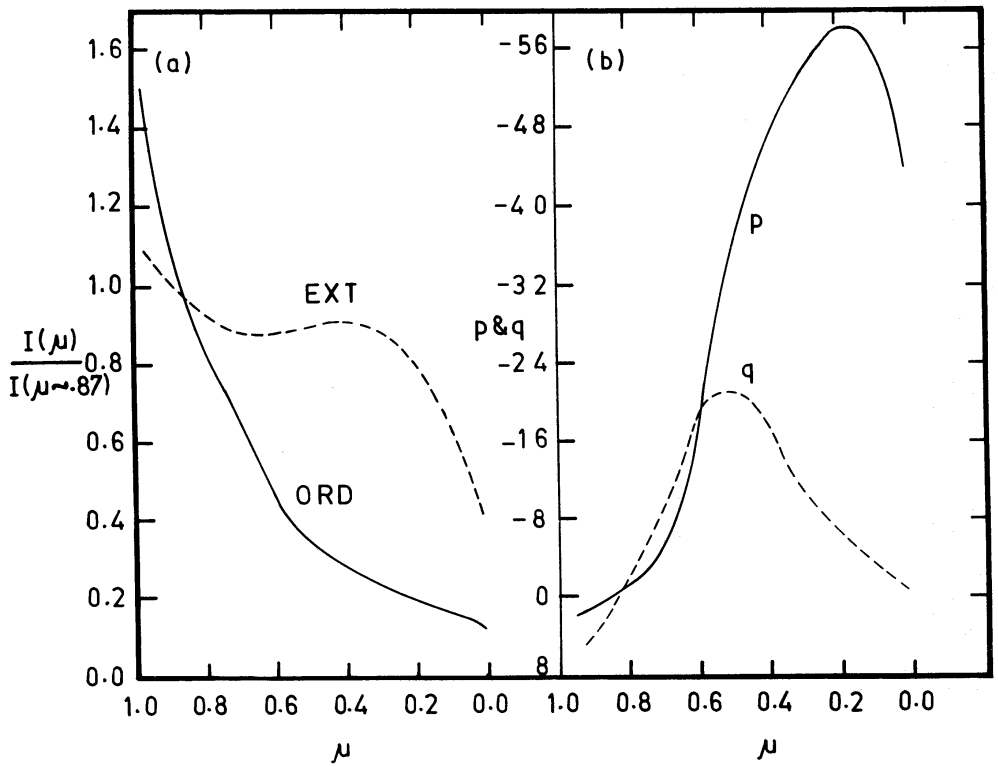

Figure 3. (a, b). The directionality of the normal wave intensities I_j/B' (normalized to their values at $\mu = 0.87$ in order to show on a linear scale), $p\,(= Q/I)$ and $q\,(= V/I)$ of the radiation emerging from a 'uniform' self-emitting plasma slab (no inputs), having the following physical conditions: $T = 10^8$ K, $(\hbar\omega/kT) = 1$; $(\hbar\omega/\hbar\omega_c) = 0.2$; $N_e = 10^{23}$ cm^{-3}. The total optical depth of the slab is 10^3.

cap emitting region of a magnetized neutron star. The ext-mode dominates because of its larger mean free path (smaller α) over the ord-mode. But more important is the effect of mode conversion scattering, by which the ordinary photons enter the ext-channel and escape easily. This process is effective because the medium is optically very thick resulting in large mean number of scatterings. For this reason, p and q [Fig. 3(b)] depend strongly on the thermal structure of the medium and the details of transfer, than on the cross-sections of the normal waves (see Meszaros & Bonazzola 1981). Fig. 4(a) corresponds to a physically identical but relatively thin slab, and hence $I_j(\mu) \propto [\alpha_j(\mu)/\mu]$ contrary to the optically thick case. The ord-wave intensity dominates because large absorption ensures large emission, and particularly because the number of scatterings is smaller in this case. Clearly, the radiation field 'reflects' the strong angular anisotropy of the cross-sections, rather than the transfer effects. p and q nearly follow the same pattern [Fig. 4(b)] but the strongly linearly-polarized ord-wave dominates. A steep reduction in the cross-sections for photons travelling parallel to the field (Canuto *et al.* 1971) is responsible for the sharp intensity maximum, the 'pencil beam' (of half width $\sim 20°$) in Fig. 3(a), as well as the 'hollow pencil beam', an intensity minimum in Fig. 4(a), for very small angles of propagation. Unlike the case of magnetic white dwarfs, p is very strong in these objects (see also Kaminker *et al.* 1982). For an irradiated magnetized slab, the results are quantitatively different. This polarized beaming (directionality) of radiation is useful in constructing the pulse shapes of X-ray pulsars, exploiting the strong dependence of the directional diagram on ω/ω_c and ξ (see Nagel 1981; Meszaros 1982 and Silant'ev 1982).

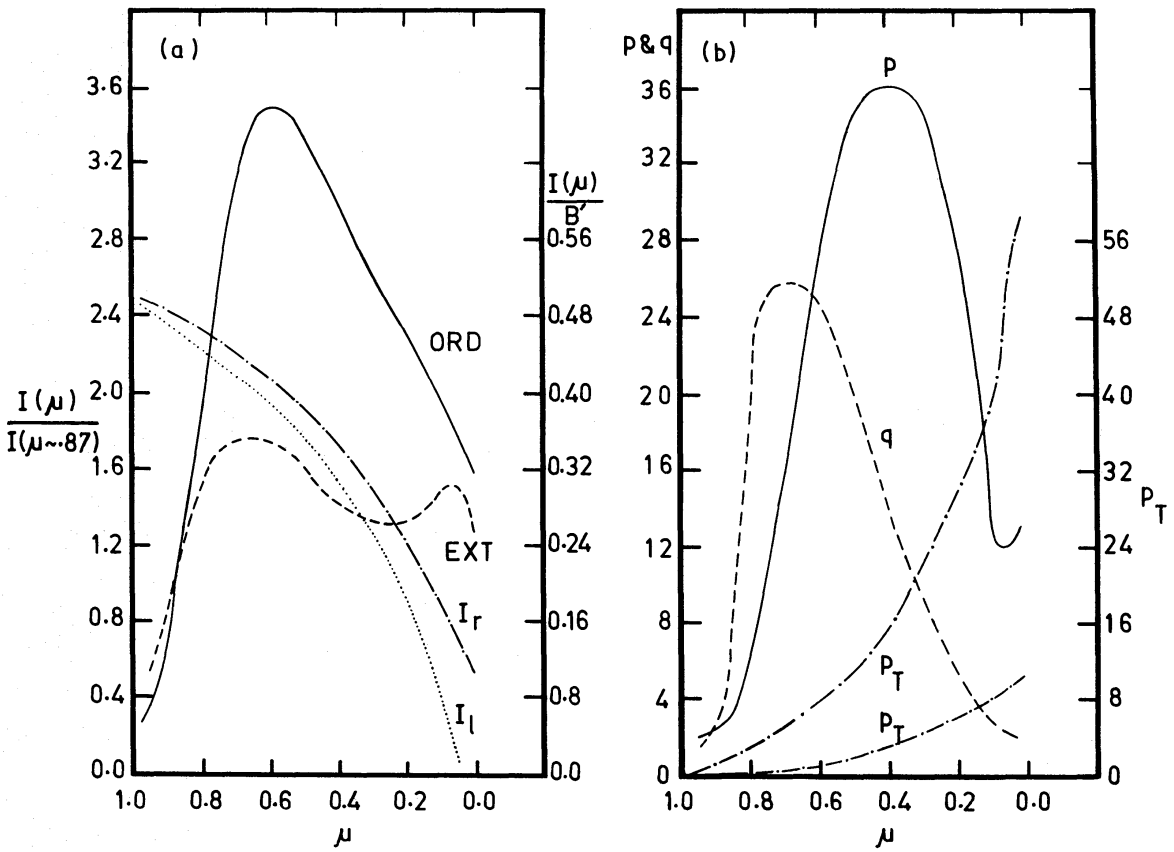

Figure 4. (a, b). Same as Fig. 3 except the total optical depth which is now taken as 10. The scale on the left refers to normal waves. The angular distribution of the intensity components $I_{l,r}/B'$ (dot and dot-dash lines) computed for the non-magnetic case, with optical depth 10, is also shown. The scale on the right refers to these results. To obtain a maximum polarization, we have taken $\bar{\omega} \equiv 1$ (i.e. conservative scattering, no internal sources), and have given an input $I_{l,r} = B' \equiv B(T)/2$ at the lower boundary. The linear polarization p_T [$= (I_r - I_l)/(I_r + I_l)$] for this Thomson scattering case reaches a maximum of approximately 10 per cent for $\mu \simeq 0$. The 'steeply rising' curve corresponds to the case when this slab is irradiated 'normally' on the free surface by a radiation field of intensity $I_{l,r}(\mu \sim 1) = B'$, again a choice producing maximum polarization. The intensity curves of this case cannot be shown in the adopted scale.

The (conservative) scattering in a non-magnetic slab of the same thickness gives rise to a smooth angular dependence for the emergent intensities $I_{l,r}$ and the linear polarization p (see Fig. 4). When this slab is illuminated on the top surface ($\tau = 0$) by a normally incident ($\mu \simeq 1$) diffuse radiation field, a large amount of linear polarization can be obtained with a steep increase near the limb. A grazing incidence for example produces a negative p. However, the detailed structure of the azimuthally dependent radiation field is qualitatively different from the azimuth-independent case, since in the former case, the coupling of p and q is stronger. For computing these later results, we have used Chandrasekhar's equations (1950, p. 43) for Rayleigh scattering polarization.

5 Solution of the Zeeman line transfer equations and test cases

Now we shall attempt to understand the advantages or otherwise of the normal wave and Stokes vector methods for this class of problems. The cold plasma normal wave equations

for Zeeman lines can be obtained from equation (1) by taking $\bar{\omega} \equiv 0$,

$$\mu \frac{dI_j}{d\tau} = k_j\left(I_j - \frac{B}{2}\right), \qquad \text{or} \qquad \mu \frac{d}{d\tau}\begin{bmatrix} I_1 \\ I_2 \end{bmatrix} = \begin{bmatrix} k_1 & 0 \\ 0 & k_2 \end{bmatrix} \begin{bmatrix} I_1 - \frac{B}{2} \\ I_2 - \frac{B}{2} \end{bmatrix} \tag{39}$$

where, now

$$k_j(\xi) = \frac{1}{\rho} \sum_{\alpha=-1}^{+1} t_\alpha^2 k^{(\alpha)} a_\alpha^j(\xi) = \sum_{\alpha=-1}^{+1} T_\alpha(\omega) a_\alpha^j(\xi), \tag{40}$$

t_α being the eigenvalues of the 'atomic' polarizability tensor. Explicit expressions can be found for $T_\alpha(\omega)$ and the line transfer coefficients in Dolginov & Pavlov (1974) and Pavlov (1975). The boundary conditions are

$$I_j(\tau_{\max}) = \frac{B(\tau_{\max})}{2}\left[1 + \beta \frac{\mu}{k_j}\right], \qquad \beta = \frac{1}{B(\tau_{\max})}\left[\frac{\partial B(\tau)}{\partial T(\tau)} \frac{\partial T(\tau)}{\partial \tau}\right]. \tag{41}$$

The Stokes vector equation for the Zeeman lines, in the usual notation, is

$$\mu \frac{d}{d\tau}\begin{bmatrix} I \\ Q \\ U \\ V \end{bmatrix} = \begin{bmatrix} \eta_I & \eta_Q & 0 & \eta_V \\ \eta_Q & \eta_I & -\rho_R & 0 \\ 0 & \rho_R & \eta_I & -\rho_W \\ \eta_V & 0 & \rho_W & \eta_I \end{bmatrix} \begin{bmatrix} I - B \\ Q \\ U \\ V \end{bmatrix}. \tag{42}$$

For further details regarding this equation, see Wittmann (1974); Martin & Wickramasinghe

Table 1. Unno atmosphere with a linear source function $B = 1 + 0.2\tau$ for the given values of constant opacities η_r and $\eta_p = \eta_I = 1$.

		Runge-Kutta	Martin & Wickramasinghe	Stokes vector representation	Normal wave representation
$\rho_R = 0$; $\rho_W = 0$; U≡O					
$\eta_r = 1$	I	1.16000	1.16000	1.16000	1.16000
$\eta_r = 1.1$	I	1.15427	1.15445	1.15445	1.15434
	Q	.00190	.00190	.00190	.00190
	V	-.00521	-.00521	-.00521	-.00521
$\eta_r = 2$	I	1.12566	1.12585	1.12585	1.12585
	Q	.01169	.01169	.01169	.01169
	V	-.03209	-.03209	-.03209	-.03209
$\eta_r = 100001$	I	-	1.08000	1.08000	1.08251
	Q	-	.02738	.02738	.02825
	V	-	-.07517	-.07517	-.07757
$\rho_R = 1.5$; $\rho_W = 0.75$					
$\eta_r = 2$	I	1.12256	1.12276	1.12276	-
	Q	.00855	.00855	.00855	-
	U	-.00836	-.00836	-.00836	-
	V	-.02482	-.02482	-.02482	-

(1981, 1982); Nagendra & Peraiah (1984). The boundary conditions are given in Stenflo (1971), and Martin & Wickramasinghe 1979, p. 886.

Test cases: For a discussion of the accuracy of the solution method, we have selected some test cases from Martin & Wickramasinghe (1979), which has to be seen for details of

Table 2. A grey atmosphere, temperature structure $T = T_e\,(0.75\,\tau + 0.5)^{1/4}$ for different constant opacities η_r and $\eta_p = \eta_l = 1$.

		Runge-Kutta	Martin & Wickramasinghe	Stokes vector representation	Normal wave representation
$\rho_R = 0;\ \rho_W = 0;\ U \equiv 0$					
$\eta_r = 1$	I	1.66270	1.66320	1.66378	1.66328
$\eta_r = 1.1$	I	1.64428	1.64481	1.64535	1.64487
	Q	.00630	.00629	.00631	.00630
	V	-.01730	-.01728	-.01732	-.01730
$\eta_r = 2$	I	1.54135	1.54196	1.54228	1.54189
	Q	.04153	.04150	.04158	.04150
	V	-.11401	-.11391	-.11415	-.11406
$\eta_r = 10001$	I	-	1.33161	1.33160	1.33888
	Q	-	.11350	.11359	.11499
	V	-	-.31157	-.31160	-.31714
$\rho_R = 1.5;\ \rho_W = 0.75$					
$\eta_r = 2$	I	1.53306	1.53375	1.53405	-
	Q	.03466	.03464	.03468	-
	U	-.02477	-.02476	-.02480	-
	V	-.09218	-.09212	-.09226	-

Table 3. A realistic model atmosphere from Wickramasinghe (1972), $T_e = 12\,000$ K for τ-dependent opacities $\eta_p = \eta_l = \eta$ with $\eta = 0.2 + \tau$.

		Runge-Kutta	Martin & Wickramasinghe	Stokes vector representation	Normal wave representation
$\rho_R = 0;\ \rho_W = 0;\ U \equiv 0$					
$\eta_r = 1\eta$	I	2.98068	2.97477	2.98229	2.97047
$\eta_r = 1.1\eta$	I	2.95500	2.94920	2.95658	2.94474
	Q	.00879	.00875	.00880	.00870
	V	-.02412	-.02403	-.02415	-.02417
$\eta_r = 2\eta$	I	2.79155	2.78625	2.79293	2.78140
	Q	.06473	.06453	.06481	.06471
	V	-.17770	-.17713	-.17792	-.17764
$\eta_r = 10001\,\eta$	I	-	1.98794	1.99154	1.99295
	Q	-	.33778	.33911	.34051
	V	-	-.92722	-.93090	-.93460
$\rho_R = 1.5;\ \rho_W = 0.75$					
$\eta_r = 2\eta$	I	2.78459	2.77945	2.78606	-
	Q	.05787	.05809	.05828	-
	U	-.06609	-.06537	-.06598	-
	V	-.13551	-.13541	-.13586	-

Table 4. Accuracy and specific times t (in seconds) on IBM 370/155, required for obtaining a solution $(IQUV)^T$. For all the cases $\mu = 0.8$, $\xi = 0.7$, $\cos 2\chi = 0.6$.

Positions		Unno/ exact	Beckers/ RK	Variable step RK	DSM-Stokes
Inside the line: Unno atmosphere $B=1+0.2\tau$, $\eta_p=\eta_l=1$, $\eta_r=2$, $\rho_R=1.5$, $\rho_W=.75$	I	1.12276	1.12276	1.12268	1.12276
	Q	.00855	.00855	.00852	.00855
	U	-.00836	-.00836	-.00837	-.00836
	V	-.02482	-.02482	-.02476	-.02482
	t	0.05	40	10	0.9
Inside the line: Real atmosphere. $\eta_p=\eta_l=\eta$, $\eta_r=2\eta$, $\eta=0.2+\tau$, $\rho_R=1.5$, $\rho_W=.75$	I	-	2.78459	2.78657	2.78606
	Q	-	.05787	.05768	.05828
	U	-	-.06609	-.06585	-.06598
	V	-	-.13551	-.13535	-.13586
	t	-	40	10	0.9
Continuum: Unno atmosphere $B=1+0.2\tau$, $\eta_p=1$, $\eta_l=.95$, $\eta_r=1.04$, $\rho_R=-.75$, $\rho_W=-.01$	I	1.16076	1.16076	1.16041	1.16076
	Q	-.00004	-.00004	-.00004	-.00004
	U	-.00016	-.00016	-.00016	-.00016
	V	-.00508	-.00508	-.00505	-.00507
	t	0.05	40	7	0.7
Continuum: Real atmosphere $\eta_p=1+.1\tau$, $\eta_l=.95+.106\tau$, $\eta_r=1.04+.0952\tau$, $\rho_R=-.75$, $\rho_W=-.01$	I	-	2.60191	2.60171	2.60125
	Q	-	-.00036	-.00036	-.00036
	U	-	-.00092	-.00091	-.00091
	V	-	-.02641	-.02634	-.02630
	t	-	40	7	0.7

Martin–Wickramasinghe (MW) and Runge–Kutta (RK) solutions. Equations (39) and (42) are solved by employing the discrete space method (DSM) of Section 3, replacing $\bar{\omega} \equiv 0$, and using $\tau \leqslant \tau_{\text{crit}} = \text{Min}\,(2\,\mathbf{MA}^{-1})$.

The solutions obtained in both the Stokes vector and normal wave representations are fairly accurate, but the accuracy of the latter depends on the field strength and the positions in the Zeeman components, unlike the former. Beckers' (1969) method which is basically an RK scheme offers the most accurate solutions for the weak lines. The variable step RK (see Landi Degl' Innocenti 1976) is faster. We have used a step size criterion based on physical arguments, given by the above author, with an accuracy index of six (an accuracy up to 10^{-6}). The average computing times (in seconds, see Tables 1–3) to obtain a solution $(I\,Q\,U\,V)^T$ are: Beckers/RK (36), variable step RK (9), MW (0.35), DSM-Stokes (0.8), DSM-normal wave (0.5). For scattering solutions (with $J = 7$), the time required is 3 min for $\tau = 10$ and 7 min for $\tau = 10^3$.

6 Conclusions

We have described an explicit numerical scheme which is useful in polarization transfer problems.

For weaker magnetic fields, the spectra and polarization of hot white dwarf atmospheres do not differ much from the results of magneto-absorption theory, because of the large

densities involved. This is not so in very strong magnetic fields and/or very hot plasmas, such as are found near accreting magnetized neutron stars, because of a strong anisotropy. Nevertheless even for weak fields a larger amount of linear polarization can be generated, in irradiated atmospheres, or by changed source function gradients. The circular polarization is rather insensitive to these changes and depends mainly on the field strength and its geometry. These preliminary results are useful in understanding the basic features of the polarized radiation fields emitted by these objects.

Acknowledgments

One of us (KNN) would like to thank D. Mohan Rao for useful discussions and comments. We are grateful to the referee for his useful comments and suggestions.

References

Beckers, J. M., 1969. *Sol. Phys.*, **9**, 372.
Canuto, V., Lodenquai, J. & Ruderman, M., 1971. *Phys. Rev. D*, **3**, 2303.
Chandrasekhar, S., 1950. *Radiative Transfer*, Oxford University Press.
Dolginov, A. Z., Gnedin, Yu. N. & Silant'ev, N. A., 1970. *J. quantit. Spectrosc. radiat. Transfer*, **10**, 707.
Dolginov, A. Z. & Pavlov, G. G., 1974. *Soviet Astr.*, **17**, 485.
Gehrels, T., 1974. *Planets Stars and Nebulae – Studied with Photopolarimetry, IAU Colloq. No. 23*, ed. Gehrels, T., University of Arizona Press.
Ginzburg, V. L., 1964. *The Propagation of Electromagnetic Waves in Plasmas*, Pergamon Press, Oxford.
Gnedin, Yu. N. & Pavlov, G. G., 1974. *Soviet Phys., JETP*, **38**, 903.
Gnedin, Yu. N. & Sunyaev, R. A., 1974a. *Soviet Phys., JETP*, **38**, 51.
Gnedin, Yu. N. & Sunyaev, R. A., 1974b. *Astr. Astrophys.*, **36**, 379.
Grant, I. P. & Hunt, G. E., 1968a. *Mon. Not. R. astr. Soc.*, **141**, 27.
Grant, I. P. & Hunt, G. E., 1968b. *J. Quantit. Spectrosc. Radiat. Transfer*, **8**, 1817.
Grant, I. P. & Hunt, G. E., 1969a. *Proc. R. Soc. Lond.*, **A313**, 183.
Grant, I. P. & Hunt, G. E., 1969b. *Proc. R. Soc. Lond.*, **A313**, 199.
Hardorp, J., Shore, S. N. & Wittmann, A., 1976. *Physics of Ap Stars*, p. 419, eds Weiss, W. W., Jenkner, H. & Wood, H. J., Universitätssternwarte Wien, Vienna.
Kaminker, A. D., Pavlov, G. G. & Shibanov, Yu. A., 1982. *Astrophys. Space Sci.*, **86**, 249.
Lamb, F. K. & ter Haar, D., 1971. *Phys. Repts*, 2C.1.
Landi Degl' Innocenti, E., 1976. *Astr. Astrophys. Suppl.*, **25**, 379.
Liebert, J., Schmidt, G. D., Green, R. F., Stockman, H. S. & Mc-Graw, J. T., 1983. *Astrophys. J.*, **264**, 262.
Martin, B. & Wickramasinghe, D. T., 1979. *Mon. Not. R. astr. Soc.*, **189**, 883.
Martin, B. & Wickramasinghe, D. T., 1981. *Mon. Not. R. astr. Soc.*, **196**, 23.
Martin, B. & Wickramasinghe, D. T., 1982. *Mon. Not. R. astr. Soc.*, **200**, 993.
Melrose, D. B., 1980. *Plasma Astrophysics*, Vol. 1, Gordon & Breach, New York.
Meszaros, P. & Bonazzola, S., 1981. *Astrophys. J.*, **251**, 695.
Meszaros, P., 1982. *Proc. International Workshop on Accreting Neutron Stars*, eds Brinkmann, W. & Trumper, J., MPE Report 177, Garching, West Germany.
Meszaros, P., 1984. *Space Sci. Rev.*, **38**, 325.
Nagel, W., 1981. *Astrophys. J.*, **251**, 278.
Nagel, W. & Ventura, J., 1983. *Astr. Astrophys.*, **118**, 66.
Nagendra, K. N. & Peraiah, A., 1984. *Astrophys. Space Sci.*, **104**, 61.
Pacholczyk, A. G., 1977. *Radio Galaxies*, Pergamon Press, Oxford.
Pavlov, G. G., 1973. *Soviet Astr.*, **17**, 209.
Pavlov, G. G., 1975. *Astrofizika*, **11**, 77.
Pavlov, G. G. & Shibanov, Yu. A., 1978. *Soviet Astr.*, **22**, 214.
Pavlov, G. G. & Panov, A. N., 1976. *Soviet Phys., JETP*, **44**, 300.
Peraiah, A. & Grant, I. P., 1973. *J. Inst. Maths. Applics.*, **12**, 75.
Peraiah, A., 1984. *Methods in Radiative Transfer*, ed. Kalkofen, W., Cambridge University Press.
Schmid-Burgk, J. & Wehrse, R., 1976. *Second European Workshop on White Dwarfs*, Observatorio Astronomico di Roma.

Silant'ev, N. A., 1982. *Astrophys. Space Sci.*, **82,** 363.
Shipman, H. L., 1971. *Astrophys. J.*, **167,** 165.
Stenflo, J. O., 1971. *Solar Magnetic Fields, IAU Symp. No. 43*, p. 101, ed. Howard, R., Reidel, Dordrecht, Holland.
Stepanov, V. E., 1958. *Izv. Krymsk. Astrofiz. Obs.*, **18,** 136.
Unno, W., 1956. *Publs astr. Soc. Japan,* **8,** 108.
van de Hulst, H. C., 1980. *Multiple Light Scattering,* Academic Press, New York.
Ventura, J., 1973. *Phys. Rev. A,* **8,** 3021.
Ventura, J., 1979. *Phys. Rev. D,* **19,** 1684.
Wesemael, F., Auer, L. H., van Horn, H. M. & Savedoff, M. P., 1980. *Astrophys. J. Suppl.*, **43,** 159.
Wickramasinghe, D. T., 1972. *Mem. R. astr. Soc.*, **76,** 129.
Wiscombe, W. J., 1976a. *J. Quantit. Spectrosc. Radiat. Transfer,* **16,** 477.
Wiscombe, W. J., 1976b. *J. Quantit. Spectrosc. Radiat. Transfer,* **16,** 637.
Wittmann, A., 1974. *Sol. Phys.*, **35,** 11.
Zheleznyakov, V. V., 1970. *Radio Emission of Sun and Planets,* Pergamon Press, New York.

Appendix: Computation of transmission and reflection matrices and source vectors

Define

$$\mathbf{Q}^{++}_{n+1/2} = \bar{\omega}_{n+1/2}\mathbf{P}^{++}_{n+1/2}\mathbf{G}; \qquad \mathbf{Q}^{+-}_{n+1/2} = \bar{\omega}_{n+1/2}\mathbf{P}^{+-}_{n+1/2}\mathbf{G};$$
$$\mathbf{Q}^{--}_{n+1/2} = \bar{\omega}_{n+1/2}\mathbf{P}^{--}_{n+1/2}\mathbf{G}; \qquad \mathbf{Q}^{-+}_{n+1/2} = \bar{\omega}_{n+1/2}\mathbf{P}^{-+}_{n+1/2}\mathbf{G} \tag{A1}$$

and then

$$\mathbf{S}^{++} = \mathbf{M} - \tfrac{1}{2}\tau_{n+1/2}(\mathbf{A}^{+}_{n+1/2} - \mathbf{Q}^{++}_{n+1/2}); \qquad \mathbf{S}^{+-} = \tfrac{1}{2}\tau_{n+1/2}\mathbf{Q}^{+-}_{n+1/2};$$
$$\mathbf{S}^{--} = \mathbf{M} - \tfrac{1}{2}\tau_{n+1/2}(\mathbf{A}^{-}_{n+1/2} - \mathbf{Q}^{--}_{n+1/2}); \qquad \mathbf{S}^{-+} = \tfrac{1}{2}\tau_{n+1/2}\mathbf{Q}^{-+}_{n+1/2} \tag{A2}$$

and

$$\boldsymbol{\Delta}^{+} = [\mathbf{M} + \tfrac{1}{2}\tau_{n+1/2}(\mathbf{A}^{+}_{n+1/2} - \mathbf{Q}^{++}_{n+1/2})]^{-1}; \qquad \boldsymbol{\Delta}^{-} = [\mathbf{M} + \tfrac{1}{2}\tau_{n+1/2}(\mathbf{A}^{-}_{n+1/2} - \mathbf{Q}^{--}_{n+1/2})]^{-1}. \tag{A3}$$

Write

$$\mathbf{r}^{+-} = \boldsymbol{\Delta}^{+}\mathbf{S}^{+-}; \qquad \mathbf{r}^{-+} = \boldsymbol{\Delta}^{-}\mathbf{S}^{-+} \tag{A4}$$

and

$$\mathbf{t}^{+} = [\mathbf{I} - \mathbf{r}^{+-}\mathbf{r}^{-+}]^{-1}; \qquad \mathbf{t}^{-} = [\mathbf{I} - \mathbf{r}^{-+}\mathbf{r}^{+-}]^{-1}, \tag{A5}$$

then, the transmission and reflection matrices are

$$\mathbf{t}(n+1, n) = \mathbf{t}^{+}[\boldsymbol{\Delta}^{+}\mathbf{S}^{++} + \mathbf{r}^{+-}\mathbf{r}^{-+}]; \qquad \mathbf{r}(n+1, n) = 2\mathbf{t}^{-}\mathbf{r}^{-+}\boldsymbol{\Delta}^{+}\mathbf{M};$$
$$\mathbf{t}(n, n+1) = \mathbf{t}^{-}[\boldsymbol{\Delta}^{-}\mathbf{S}^{--} + \mathbf{r}^{-+}\mathbf{r}^{+-}]; \qquad \mathbf{r}(n, n+1) = 2\mathbf{t}^{+}\mathbf{r}^{+-}\boldsymbol{\Delta}^{-}\mathbf{M} \tag{A6}$$

and, the source vectors are

$$\boldsymbol{\Sigma}^{+}(n+1, n) = (1 - \bar{\omega}_{n+1/2})\tau_{n+1/2}\mathbf{t}^{+}[\boldsymbol{\Sigma}^{+}_{n+1/2} + \mathbf{r}^{+-}\boldsymbol{\Delta}^{-}\boldsymbol{\Sigma}^{-}_{n+1/2}]$$
$$\boldsymbol{\Sigma}^{-}(n, n+1) = (1 - \bar{\omega}_{n+1/2})\tau_{n+1/2}\mathbf{t}^{-}[\boldsymbol{\Delta}^{-}\boldsymbol{\Sigma}^{-}_{n+1/2} + \mathbf{r}^{-+}\boldsymbol{\Delta}^{+}\boldsymbol{\Sigma}^{+}_{n+1/2}] \tag{A7}$$

where

$$\boldsymbol{\Sigma}^{+}_{n+1/2} = \bar{\omega}_{n+1/2}\tau_{n+1/2}\mathbf{P}^{+}_{*n+1/2}\mathbf{I}^{+}_{*}\frac{\exp(-\tau_n/\mu_0)}{2}[\exp(-\tau_{n+1/2}/\mu_0) + 1] + \mathbf{A}^{+}_{a,\,n+1/2}\mathbf{B}^{+}_{n+1/2}$$

$$\boldsymbol{\Sigma}^{-}_{n+1/2} = \bar{\omega}_{n+1/2}\tau_{n+1/2}\mathbf{P}^{-+}_{*n+1/2}\mathbf{I}^{+}_{*}\frac{\exp(-\tau_n/\mu_0)}{2}[\exp(-\tau_{n+1/2}/\mu_0) + 1]$$
$$+ \mathbf{A}^{-}_{a,\,n+1/2}\mathbf{B}^{-}_{n+1/2}. \tag{A8}$$